nature geoscience

PERSPECTIVE

PUBLISHED ONLINE: 10 APRIL 2017 | DOI: 10.1038/NGEO2922

The cold and relatively dry nature of mantle forearcs in subduction zones

G. A. Abers[1]*, P. E. van Keken[2] and B. R. Hacker[3]

Some of Earth's coldest mantle is found in subduction zones at the tip of the mantle wedge that lies between the subducting and overriding plates. This forearc mantle is isolated from the flow of hot material beneath the volcanic arc, and so is inferred to reach temperatures no more than 600 to 800 °C — conditions at which hydrous mantle minerals should be stable. The forearc mantle could therefore constitute a significant reservoir for water if sufficient water is released from the subducting slab into the mantle wedge. Such a reservoir could hydrate the plate interface and has been invoked to aid the genesis of megathrust earthquakes and slow slip events. Our synthesis of results from thermal models that simulate the conditions for subduction zones globally, however, indicates that dehydration of subducting plates is too slow over the life span of a typical subduction zone to hydrate the forearc mantle. Hot subduction zones, where slabs dehydrate rapidly, are an exception. The hottest, most buoyant forearcs are most likely to survive plate collisions and be exhumed to the surface, so probably dominate the metamorphic rock record. Analysis of global seismic data confirms the generally dry nature of mantle forearcs. We conclude that many subduction zones probably liberate insufficient water to hydrate the shallower plate boundary where great earthquakes and slow slip events nucleate. Thus, we suggest that it is solid-state processes and not hydration that leads to weakening of the plate interface in cold subduction zones.

Subduction zones produce voluminous mantle-sourced magmas. This requires that the mantle temperatures below volcanic arcs are sufficiently high for melting of hydrated peridotite[1]. However, low heat flow and seismic attenuation indicate that the shallow parts of mantle forearcs are cold and cannot be engaged in the mantle circulation beneath arcs. These data require a deep decoupling between the top of the subducted plate and the overriding mantle wedge to depths of approximately 80 km[2–4]. Hydrous minerals such as chlorite and serpentine are stable in this cold mantle forearc (Fig. 1). Low temperature alone is necessary but not sufficient for hydrous phases to be present, because enough H_2O needs to be available as well. Large H_2O fluxes are required for full hydration, because serpentinites hold 12–13 wt% H_2O (ref. 5).

Forearc H_2O storage capacity

We estimate the potential for hydration of the cold forearc mantle wedge for a global suite of 56 subduction zone thermal and petrological models[4,6,7] by comparing the H_2O flux from the slab predicted from those models with the mass of H_2O that could be stored in the cold forearc mantle. To reproduce the ubiquitous observation of low forearc heat flow and low seismic attenuation, these models decouple the subducting slab from the overlying mantle to a depth of 80 km. At greater depths, the slab is viscously coupled to the mantle wedge driving the flow of hot asthenosphere below the volcanic arc[3,4]. Tests with 70 and 100 km decoupling depths show similar patterns and negligibly different results (see Supplementary Discussion 4 for details and sensitivity tests). As a consequence, the slab surface transitions from <500 °C at <80 km depth to >800 °C at ~100 km (Fig. 2a), which is the typical depth of the slab below the volcanic arc. For the overlying mantle wedge we estimate the maximum possible mineral-bound water content for a water-saturated peridotite of composition depleted mid-ocean ridge basalt (MORB) mantle (DMM)[7,8]. Mineral assemblages at each temperature and pressure are calculated for this composition via the Gibbs free energy minimization program Perple_X[9] using the methods and phase assemblages detailed in ref. 7; Fig. 2b shows an example of the resulting H_2O content. The same approach is used to estimate devolatilization of the subducting sediment, crust and mantle, which provides estimates of H_2O fluxes from the slab[6] (Fig. 2e,f). These devolatilization models assume that all pore fluids are expelled at shallow depth.

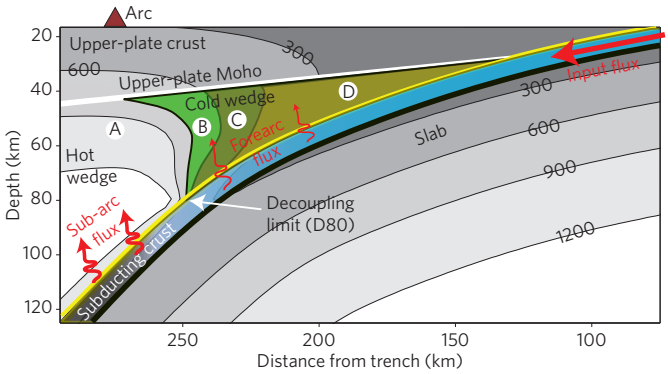

Figure 1 | Schematic forearc showing water fluxes and potentially hydrated mantle. Upper-plate mantle shows hydration variation: subarc anhydrous mantle (lherzolite) (A); potentially hydrated cold forearc (B)–(D). The facies for hydrated lherzolite are: chlorite-talc lherzolite (B); serpentine-chlorite wherlite (C); and serpentine-chlorite-brucite wherlite (D) (see Supplementary Discussion 4). The grey shades indicate temperature, labelled every 300 °C, whereas the red arrows and labels show major water fluxes mediated by subduction.

[1]Department of Earth and Atmospheric Sciences, Cornell University, 2122 Snee Hall, Ithaca, New York 14853, USA. [2]Department of Terrestrial Magnetism, Carnegie Institution for Science, 5241 Broad Branch Road NW, Washington DC 20015, USA. [3]Department of Earth Science, University of California, Santa Barbara, Santa Barbara, California 93106, USA. *e-mail: abers@cornell.edu

© 2017 Macmillan Publishers Limited, part of Springer Nature. All rights reserved.

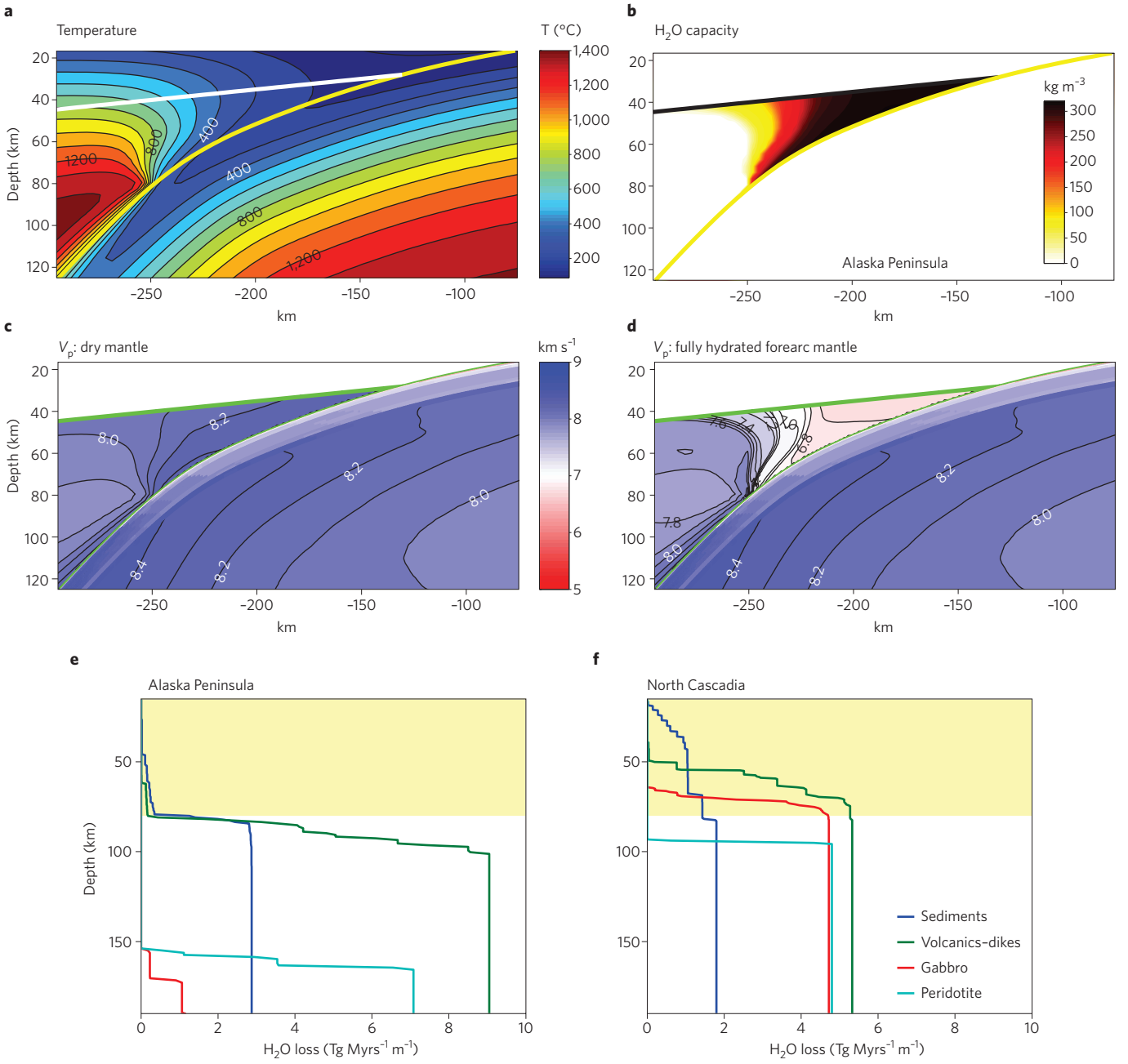

Figure 2 | Predicted hydration potential and seismic velocities for individual arcs. a–e, Alaska Peninsula example (arc 1 on Supplementary Table 1). **a**, Predicted temperatures (from ref. 4). Yellow line, modelled slab surface; white line, upper-plate Moho from compilation. **b**, Maximum water capacity in the mantle wedge predicted for a fully hydrated DMM[7] peridotite, expressed as mass of H_2O per m^3 of mantle. **c**, Predicted V_p for a dry mantle (assuming anhydrous DMM composition), mineralogy estimated as described in text, and elastic moduli following ref. 22. V_p for subducting crust has been similarly derived for hydrated compositions[6]. **d**, Predicted isotropic P-wave velocity (V_p) for a fully hydrated forearc mantle wedge (assuming water-saturated DMM composition) corresponding to hydration in **b**. Contour intervals are 0.1 km s^{-1} for **c** and **d**; lowest velocities in **d** are 6.6–6.7 km s^{-1}. **e**, Metamorphic dehydration of down-going slab versus slab surface depth for model D80[4,6], for major layers within down-going slab. The yellow field shows region below mantle forearc where vertical H_2O migration would hydrate it. **f**, Same as **e** but for North Cascadia, a hot slab with substantial dehydration beneath the mantle forearc. In all calculations the pressure is assumed to be lithostatic.

Sediment compaction occurs at depths less than 4–10 km below the sea floor and drives fluids toward the trench. These depths are generally shallower than the mantle wedge[10,11] except possibly in the Marianas where the upper plate is exceptionally thin and serpentine mud volcanoes occur[12], perhaps tapping compaction-driven fluid.

The H_2O storage capacity of the cold mantle wedge depends on its volume, which in turn depends critically on the slab geometry and the depth of the upper-plate Moho. The geometry of the slab follows refs 4,13. The upper-plate Moho geometry is estimated from a large number of seismological studies worldwide that use wide-angle marine seismic imaging, receiver functions, local earthquake tomography and gravity models (detailed in Supplementary Table 1 and the accompanying Supplementary Discussion). At many forearcs the upper-plate Moho dips away from the trench and deepens toward the volcanic arc. We have included such a sloping Moho where these observations are available.

© 2017 Macmillan Publishers Limited, part of Springer Nature. All rights reserved.

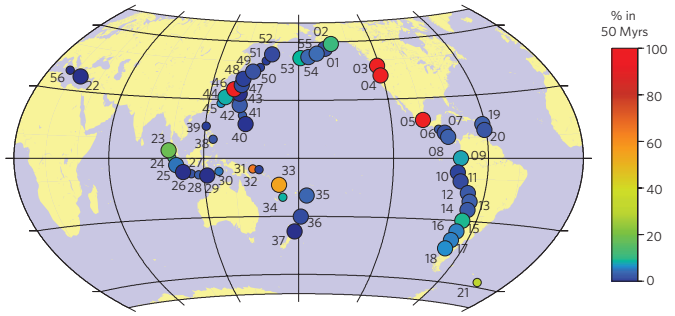

Figure 3 | Predicted per cent hydration of mantle wedges worldwide produced over last 50 Myrs. Predictions from thermal models with decoupling to 80 km and vertical water transport (Supplementary Table 2); models are steady state except where noted in Supplementary Discussion 4. The colours denote hydration, whereas larger circles show arcs with well-constrained geometry (uncertainty in forearc crustal thickness < 10 km and uncertainty in depth to slab below volcanic front[38] < 20 km). The numbers code to subduction zones listed in Supplementary Tables 1 and 2, the following of which are discussed in the main text: 1, Alaska Peninsula; 4, Cascadia; 5, Mexico; 31, New Britain; 33, North Vanuatu; 46, Nankai; 48, North Honshu.

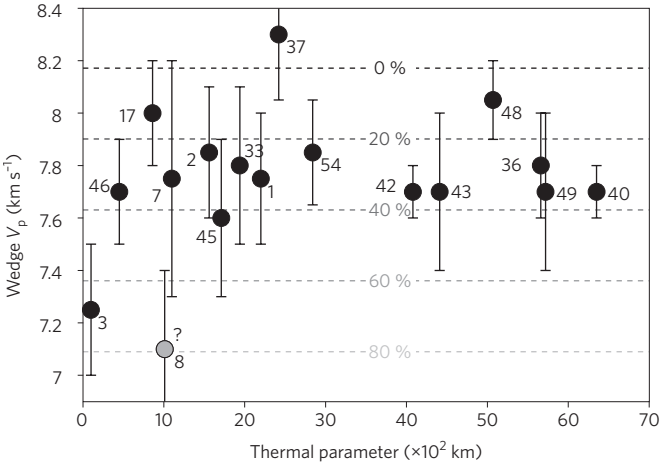

Figure 4 | Compilation of V_p observed in the shallowest parts of forearc mantle wedges versus slab thermal parameter. The thermal parameter is the product of plate convergence rate, incoming plate age, and sine of plate dip (from refs 4,6). V_p are compiled from active-source wide-angle reflections — typically just below Moho — or local earthquake travel times (Supplementary Table 3). The error bars show the approximate range in values observed in the wedge. The numbers correspond to arc sections in Supplementary Table 1. The grey circle and question mark represent Costa Rica, which shows a P-wave to S-wave velocity ratio (V_p/V_S) inconsistent with predicted hydration. Horizontal dashed lines show velocities predicted for hydration of DMM peridotite as described in text, at 40 km depth (1.2 GPa) and 400 °C, as a Hashin–Shtrikman mixture between elastic moduli of fully hydrated and dry DMM.

Predicted hydration

Based on these upper-plate Moho geometries, the slab models and the predicted water content for fully hydrated forearcs, we find that forearcs could sequester a total of 2.6×10^{10} Tg of H_2O globally, or about 2% of the mass of current global ocean water. From the slab dehydration models we estimate that 0.4×10^8 Tg per million years (Myrs) of H_2O is released beneath the forearc mantle at depths less than 80 km. This water is derived principally from subducting sediments and upper volcanic rocks (Fig. 2e) and constitutes only a small fraction of the 10^9 Tg per Myrs H_2O being subducted worldwide[6]. At this rate, it would take ~500 Myrs to saturate Earth's forearcs. However, most subduction zones remain in a stable configuration for only a few tens of Myrs. For example, the Aleutian, Mariana and northern Cascadia arcs formed no more than 50 million years ago (Ma) (refs 14–16) and the collision of the Ontong Java plateau reset arc geometries throughout Melanesia at 10–20 Ma[17]. In 50% of arcs, the forearc undergoes continuous removal by subduction erosion[18]. As a consequence, the forearc in most subduction zones should be far from saturated in H_2O.

Figure 3 compares the variability in hydration expected in 50 Myrs — assumed here as a nominal forearc age — by dividing the forearc mass available for hydration by the underlying slab dehydration rate. The majority of arcs show <10% hydration in 50 Myrs. Notable exceptions are Cascadia, Mexico and Nankai where young plate ages and slow convergence lead to unusually hot slab surfaces and significant slab dehydration at depths less than 80 km (Fig. 2f). In these endmember cases, nearly complete hydration can be expected in 50 Myrs. Our calculations also predict high hydration rates for New Britain and North Vanuatu. These two subduction zones feature relatively recent (5–20 Ma (ref. 17)) subduction below young oceanic arc lithosphere, for which our models predict a thin thermal boundary layer that leads to a rather small cold volume of the mantle wedge. Such a small cold wedge is hydrated much more rapidly than typical subduction zones and leads to unusual predictions for the few cases of nascent subduction below young oceanic lithosphere. In general the forearc mantle should be largely dry except where the youngest plates subduct.

Our predictions for the hydration state of the forearc mantle are affected by uncertainties in several assumptions that are detailed in Supplementary Discussion 2. Uncertainties in wedge geometries result in 5–15% net uncertainty in total hydration, although uncertainties at some individual arcs may be larger. Updip migration of released fluids may occur trenchward of the mantle forearc or beneath the deeper hot flowing mantle[11,19] and alter fluid budgets. Fluids released in the thrust zone updip of the mantle wedge should not affect the mantle fluid budget, although they may somewhat lower temperatures[20]. Fluids released below the arc probably travel primarily to the hot wedge, as geochemical signatures require much subduction-derived fluid to migrate to arc volcanoes[1]. As a consequence the H_2O transport from the hot wedge to the cold forearc wedge is limited. Finally, reconciling these thermal models with the exposed suites of high-pressure rocks remains a challenge since exhumed rock compositions are thought to represent generally warmer conditions than predicted by the models[21]. This may largely reflect biases in exhumed sample datasets toward buoyant and typically hotter forearcs[22].

We note that these estimates are averages over the entire forearc. It is likely that hydration varies spatially, and is highest just above the plate interface, near where H_2O enters the mantle wedge.

Comparison with seismic observations

To test these predictions for the forearc mantle hydration state, the thermal-petrologic models for each arc are used to predict forearc seismic velocities from mineralogy[23] using the approach discussed in ref. 7. The example in Fig. 2c,d shows that hydration should have a very large effect on seismic velocities in the forearc. For most cold mantle forearcs, we predict that anhydrous peridotite should have V_p of 8.0–8.4 km s^{-1}, whereas fully hydrated mantle forearcs have V_p as low as 6.6 km s^{-1}. This 20% V_p reduction should be easily detectable. Observations from local earthquake tomography and wide-angle reflection/refraction imaging (Supplementary Discussion 3 and Supplementary Table 3) show that most forearcs have a V_p of 7.6–8.0 km s^{-1}, consistent with < 20–40% hydration (Fig. 4). These estimates do not consider biases due to anisotropy

© 2017 Macmillan Publishers Limited, part of Springer Nature. All rights reserved.

in serpentinite[24]. Observed local-earthquake shear-wave splitting for signals sampling the cold parts of mantle forearcs indicate that anisotropy effects are minor. Typical splitting times of 0.06–0.15 s are compatible with only 1–2% aggregate anisotropy or less[25,26]. If free fluids were present they would further reduce velocities and produce significantly greater velocity reduction per amount of H_2O than creation of hydrous minerals[27], so that the hydration estimates on Fig. 4 would be upper bounds. However, free water should not be stable in an H_2O-undersaturated forearc mantle. Thus, most observations support the predicted weak hydration.

A significant exception to this general pattern is the Cascadia mantle forearc, which has very low V_p near 7.1 km s^{-1} and an inverted seismic Moho[28,29], consistent with the high hydration predicted from Figs 2 and 3. Hydrated forearcs are probably confined to subduction zones with young subducting plates that devolatilize quickly. Although one might predict similar hydration in Nankai (Fig. 3. and label number 46 on Fig. 4), conditions favouring early slab dehydration here have probably arisen only in the last 4 Myrs so the integrated effect should be less (See Supplementary Discussion 4). Costa Rica also shows very low V_p of 6.8–7.4 km s^{-1} in the shallowest part of the mantle wedge <50 km deep[30], but the corresponding V_p/V_s ratio in the slow part of that wedge is 1.70–1.80. These observations are inconsistent with serpentinite, which should have V_p/V_s >1.85 for rocks that have V_p < 7.4 km s^{-1}, and may instead reflect addition of crustal material from either the upper or lower plate into the shallowest mantle wedge by subduction erosion.

In general a variety of tectonic processes may mechanically mix low-velocity silicic material into the shallow part of the mantle wedge to achieve slow velocities without serpentinization. For example, it has been suggested that crust tectonically erodes or delaminates from the base of the upper plate[31], is scraped off the downgoing plate and rises as diapirs, or re-laminates the base of the upper plate[32]. Any of these processes would reduce the aggregate seismic velocity of the cold wedge, because a wide variety of mafic and intermediate-composition rock has V_p in the 7.0–7.5 km s^{-1} range[32]. The hydration estimates in Fig. 4 are thus probably overestimates and it is possible that the forearc mantle may be essentially dry, except in the warmest-slab subduction zones. More observations of V_p/V_s in mantle forearcs are needed to test this supposition.

Mechanical consequences for subduction zones

In summary, most subduction zone mantle forearcs should be only weakly hydrated (<20%) owing to low water fluxes and short durations of stable arc configurations. Only the hottest subduction zones such as Cascadia should have highly hydrated forearcs. Observations of V_p in mantle forearc wedges are consistent with these predictions. The low hydration is a result of low rates of metamorphic devolatilization of the slab beneath cold forearcs, which greatly limits the water available to migrate updip. The distribution of hydrous phases in the forearc may be uneven with higher concentrations near the plate interface.

Metamorphic fluids have been suggested to greatly elevate pore pressures along the interplate thrust zone at depths where episodic tremor and slow slip events occur[10,33] and to explain low seismic velocities along the plate interface[34]. These studies argue that overpressure creates very weak faults, facilitating transitory phenomena such as slow slip[33]. However, the availability of water in most forearcs may be too low to accommodate large high-porosity regions on the plate interface, except at the hottest subduction zones. Even if hydration is concentrated near the plate interface, the low water fluxes into the cold forearc make it difficult to sustain large porous channels of high pressure. Without large volumes of slab-derived fluid reaching 30–50 km depth, alternative explanations for these phenomena may be more likely; for example, slow slip may result from frictional instabilities in hydrous silicates[35], which in abundance may produce the observed low-velocity layers along the plate boundary without copious additional water. Again, hot subduction zones may be an exception owing to the rapid devolatilization under the forearc there.

Other geodynamic processes may be also worth reconsidering. For example, weakly hydrated forearcs should have negative to neutral buoyancy with respect to ambient mantle, with only the forearcs of hot subduction zones being positively buoyant. The hottest forearcs are therefore the least likely to founder during collisions, and more likely to be preserved in the geological record. They are also more likely to promote the exhumation of high-pressure mafic rocks emplaced beneath the forearc[36,37], perhaps explaining the systematic off-set observed between thermal models and inferred high-pressure rock temperatures[21]. Again, the hydration estimates on Fig. 4 are overestimates to the extent that free fluids are present and crustal material is embedded in the shallow forearc through material exchange between upper and lower plates[38]. Future work on this topic could address fluid sources or pathways not considered here (for example, whether fluid is derived from pore compaction in basalts at these depths or whether fluid generated at deeper levels might migrate far up the slab to enter the forearc) and the implications of tectonic erosion and other mixing processes for the composition of the forearc mantle.

Received 9 August 2016; accepted 24 February 2017; published online 10 April 2017

Data availability. All primary and derived observations come from published sources, which are detailed in Supplementary Tables 1 and 3.

Code availability. The thermal models originally published in refs 4 & 6 are available at: http://www.earth.lsa.umich.edu/~keken/subduction/global_comparison/ZIP/.

References

1. Grove, T. L., Till, C. B. & Krawczynski, M. J. The role of H_2O in subduction zone magmatism. *Annu. Rev. Earth Planet. Sci.* **40,** 413–439 (2012).
2. Abers, G. A., van Keken, P. E., Kneller, E. A., Ferris, A. & Stachnik, J. C. The thermal structure of subduction zones constrained by seismic imaging: implications for slab dehydration and wedge flow. *Earth Planet. Sci. Lett.* **241,** 387–397 (2006).
3. Wada, I. & Wang, K. Common depth of slab-mantle decoupling: reconciling diversity and uniformity of subduction zones. *Geochem. Geophys. Geosyst.* **10,** Q10009 (2009).
4. Syracuse, E. M., van Keken, P. E. & Abers, G. A. The global range of subduction zone thermal models. *Phys. Earth Planet. Int.* **183,** 73–90 (2010).
5. Reynard, B. Serpentine in active subduction zones. *Lithos* **178,** 171–185 (2013).
6. van Keken, P. E., Hacker, B. R., Syracuse, E. M. & Abers, G. A. Subduction factory 4: depth-dependent flux of H_2O from subducting slabs worldwide. *J. Geophys. Res.* **116,** B01401 (2011).
7. Hacker, B. R. H_2O subduction beyond arcs. *Geochem. Geophys. Geosyst.* **9,** Q03001 (2008).
8. Workman, R. K. & Hart, S. R. Major and trace element composition of the depleted MORB mantle (DMM). *Earth Planet. Sci. Lett.* **231,** 53–72 (2005).
9. Connolly, J. A. D. Computation of phase equilibria by linear programming: a tool for geodynamic modeling and its application to subduction zone decarbonation. *Earth Planet. Sci. Lett.* **236,** 524–541 (2005).
10. Saffer, D. M. & Tobin, H. J. Hydrogeology and mechanics of subduction zone forearcs: fluid flow and pore pressure. *Annu. Rev. Earth Planet. Sci.* **39,** 157–186 (2011).
11. Jarrard, R. D. Subduction fluxes of water, carbon dioxide, chlorine and potassium. *Geochem. Geophys. Geosyst.* **4,** GC000392 (2003).
12. Fryer, P., Wheat, C. G. & Mottl, M. J. Mariana blueschist mud volcanism: implications for conditions within the subduction zone. *Geology* **27,** 103–106 (1999).
13. Syracuse, E. M. & Abers, G. A. Global compilation of variations in slab depth beneath arc volcanoes and implications. *Geochem. Geophys. Geosyst.* **7,** Q05017 (2006).
14. Jicha, B. R., Scholl, D. W., Singer, B. S., Yogodzinski, G. M. & Kay, S. M. Revised age of Aleutian island arc formation implies high rate of magma production. *Geology* **34,** 661–664 (2006).

© 2017 Macmillan Publishers Limited, part of Springer Nature. All rights reserved.

15. Reagan, M. K. *et al.* Fore-arc basalts and subduction initiation in the Izu–Bonin–Mariana system. *Geochem. Geophys. Geosyst.* **11,** GC002871 (2010).
16. Wells, R. *et al.* Geologic history of Siletzia, a large igneous province in the Oregon and Washington Coast Range: correlation to the geomagnetic polarity time scale and implications for a long-lived Yellowstone hotspot. *Geosphere* **10,** 692–719 (2014).
17. Hall, R. Cenozoic geological and plate tectonic evolution of SE Asia and the SW Pacific: computer-based reconstructions, model and animations. *J. Asian Earth Sci.* **20,** 353–431 (2002).
18. Clift, P. & Vannucchi, P. Controls on tectonic accretion versus erosion in subduction zones: implications for the origin and recycling of the continental crust. *Rev. Geophys.* **42,** RG2001 (2004).
19. Wilson, C. R., Spiegelman, M., van Keken, P. E. & Hacker, B. R. Fluid flow in subduction zones: the role of solid rheology and compaction pressure. *Earth Planet. Sci. Lett.* **401,** 261–274 (2014).
20. Cozzens, B. D. & Spinelli, G. A. A wider seismogenic zone at Cascadia due to fluid circulation in subducting oceanic crust. *Geology* **40,** 899–902 (2012).
21. Penniston-Dorland, S. C., Kohn, M. J. & Manning, C. E. The global range of subduction zone thermal structures from exhumed blueschists and eclogites: rocks are hotter than models. *Earth Planet. Sci. Lett.* **428,** 243–254 (2015).
22. Spandler, C. & Pirard, C. Element recycling from subducting slabs to arc crust: a review. *Lithos* **170–171,** 208–223 (2013).
23. Abers, G. A. & Hacker, B. R. A MATLAB toolbox and Excel workbook for calculating the densities, seismic wave speeds, and major element composition of minerals and rocks at pressure and temperature. *Geochem. Geophys. Geosyst.* **17,** GC006171 (2016).
24. Brownlee, S. J., Hacker, B. R., Harlow, G. E. & Seward, G. Seismic signatures of a hydrated mantle wedge from antigorite crystal-preferred orientation (CPO). *Earth Planet. Sci. Lett.* **375,** 395–407 (2013).
25. Yang, X., Fischer, K. M. & Abers, G. A. Seismic anisotropy beneath the Shumagin Islands segment of the Aleutian-Alaska subduction zone. *J. Geophys. Res.* **100,** 18165–118177 (1995).
26. Nakajima, J. & Hasegawa, A. Shear-wave polarization anisotropy and subduction-induced flow in the mantle wedge of northeastern Japan. *Earth Planet. Sci. Lett.* **225,** 365–377 (2004).
27. Korenaga, J. On the extent of mantle hydration caused by plate bending. *Earth Planet. Sci. Lett.* **457,** 1–9 (2017).
28. Bostock, M. G., Hyndman, R. D., Rondenay, S. & Peacock, S. M. An inverted continental Moho and serpentinization of the forearc mantle. *Nature* **417,** 536–538 (2002).
29. Brocher, T. M., Parsons, T., Trehu, A. M., Snelson, C. M. & Fisher, M. A. Seismic evidence for widespread serpentinized forearc upper mantle along the Cascadia margin. *Geology* **31,** 267–270 (2003).
30. DeShon, H. *et al.* Seismogenic zone structure beneath the Nicoya Peninsula, Costa Rica, from three-dimensional local earthquake *P*- and *S*-wave tomography. *Geophys. J. Int.* **164,** 109–124 (2006).
31. Kay, R. W. & Kay, S. M. Delamination and delamination magmatism. *Tectonophysics* **219,** 177–189 (1993).
32. Hacker, B. R., Kelemen, P. B. & Behn, M. D. Continental lower crust. *Annu. Rev. Earth Planet. Sci.* **43,** 167–205 (2015).
33. Liu, Y. J. & Rice, J. R. Spontaneous and triggered aseismic deformation transients in a subduction fault model. *J. Geophys. Res.* **112,** JB004930 (2007).
34. Audet, P., Bostock, M. G., Christensen, N. I. & Peacock, S. M. Seismic evidence for overpressured subducted oceanic crust and sealing of the megathrust. *Nature* **457,** 76–78 (2009).
35. Leeman, J., Saffer, D., Scuderi, M. & Marone, C. Laboratory observations of slow earthquakes and the spectrum of tectonic fault slip modes. *Nat. Commun.* **7,** 11104 (2016).
36. Guillot, S., Hattori, K. H. & de Sigoyer, J. Mantle wedge serpentinization and exhumation of eclogites: insights from eastern Ladakh, northwest Himalaya. *Geology* **28,** 199–202 (2000).
37. Schwartz, S., Allemand, P. & Guillot, S. Numerical model of the effect of serpentinites on the exhumation of eclogitic rocks: insights from the Monviso ophiolitic massif (Western Alps). *Tectonophysics* **342,** 193–206 (2001).
38. Hacker, B. R., Kelemen, P. B. & Behn, M. D. Differentiation of the continental crust by relamination. *Earth Planet. Sci. Lett.* **307,** 501–516 (2011).

Acknowledgments

This work is funded by NSF awards OCE-1446970 to GAA, OCE-1249353 and OCE-1356132 to P.E.v.K., and EAR-1249703 to B.R.H.

Author contributions

GA compiled and analysed seismic data, P.E.v.K. oversaw geodynamic modelling, B.R.H. oversaw petrology and thermodynamic modelling. All of the authors contributed to discussion and writing of the manuscript.

Additional information

Supplementary information is available in the online version of the paper. Reprints and permissions information is available online at www.nature.com/reprints. Publisher's note: Springer Nature remains neutral with regard to jurisdictional claims in published maps and institutional affiliations. Correspondence should be addressed to G.A.A.

Competing financial interests

The authors declare no competing financial interests.

© 2017 Macmillan Publishers Limited, part of Springer Nature. All rights reserved.